A Control Algorithm of an Idle Stop and Go System With Traffic Conditions for Hybrid Electric Vehicles

Kyuhyun Sim and Sung-Ho Hwang, *Member, IEEE*

***Abstract*— This paper proposes a control algorithm for IGS (Idle Stop and Go) systems and a stop prediction algorithm. A new ISG system has been introduced to reduce fuel consumption by improving the conventional ISG system for hybrid electric vehicles (HEVs), including plug-in hybrid electric vehicles (PHEVs). When the HEVs stop or pass in front of a traffic light, the control algorithm determines when to turn off the internal combustion engine (ICE) while comparing the driving energy consumption. A stop prediction algorithm was proposed to determine whether a vehicle will stop at traffic lights. Traffic information and driving test results were obtained using a driver-in-the-loop simulator, and the stop prediction algorithm was verified through these results. The proposed ISG with the stop prediction function can reduce fuel consumption. With the developed traffic flow model, the effectiveness of the proposed ISG was evaluated in terms of the transportation system.**

***Index Terms*— Idle stop and go system, traffic signal, hybrid electric vehicle, stop prediction, traffic flow model, driver-in-the-loop simulation.**

I. Introduction

CONVENTIONAL vehicles with only an internal combustion engine (ICE) use an idle stop and go system (ISG) to reduce fuel consumption and pollution in various situations. The ISG system uses an idle stop state in which the engine automatically stops for a few seconds when a vehicle stops and the brake pedal is depressed [1]. However, if traffic signals change immediately from a red light to green light when the vehicle stops, the ISG is not helpful; this is because the engine must stop for several seconds to reduce fuel consumption and pollution [2]. Therefore, traffic signal information can solve this problem for a basic ISG system. There have been many studies that reduces driving energies by controlling vehicle speed under given traffic signal conditions [3], [4], but few studies have been to improve an ISG system.

The U.S. Department of Transportation describes an application program for connected vehicles that consists of a connected car and intelligent transport system (ITS) services, including vehicle-to-infrastructure (V2I), vehicle-to-vehicle (V2V) safety services, emergency data transmission services, and eco-friendly driving assistance services [5]. In Europe, the DRIVE C2X project established seven national test sites and a harmonized testing environment for C2X technologies to accelerate cooperative mobility [6]. An ISG system using V2I communication has been investigated [7]. When engine stop time and traffic signals are predicted, this method can improve the ISG system. However, it has limits in which the traffic signals and engine stop time must fit properly. Specifically, if the engine stop time is short, an unnecessary fuel consumption occurs because the ICE turns on. In this research, a hybrid electric vehicle (HEV) system addressed the limitations by using mode transition. The objective is to propose an ISG system with traffic conditions by predicting vehicle deceleration. The control algorithm stops the ICE and switches the electric driving mode from the hybrid driving mode for a predicted deceleration section. Our previous research has been published [8]. This paper designs the proposed control algorithm and verifies its effectiveness with simulation methods.

Driver-in-the-loop simulation is that a driver drives a vehicle in virtual driving environment. Specifically, it is suitable that the simulation can control the virtual transportation system and receive the data of subjective vehicle, traffic signals, and surrounding vehicles. It also repeatedly simulates the same conditions. The developed driver-in-the-loop simulator with the powertrain model evaluates the ISG system.

A conventional ISG is operated during braking and stop situations. In this research, the HEV turns off the ICE when braking. To develop a control algorithm with traffic signals, an ISG algorithm is proposed that includes the conventional ISG system of the HEV. Driving condition were divided into four sections, as shown in Fig. 1. The first section is hybrid driving mode which operates the electric motor and ICE. The second section is regenerative braking when the vehicle decelerates. The conventional HEV turns off the ICE unless the charge state of the battery is low. The third section is when the vehicle stops because a traffic signal is red. The final section is when the vehicle starts and speeds up when the traffic signal is green. In the second and third sections, the ICE turns off. We will validate the ISG with the developed simulation environments.

The paper is organized as follows. Section 2 proposes a control algorithm of the ISG system with traffic signals. Section 3 describes stop prediction algorithm for the ISG control algorithm. Sections 4 simulates the ISG control

Manuscript received 24 October 2019; revised 20 April 2020, 11 October 2020, 16 March 2021, and 7 November 2021; accepted 9 November 2021. Date of publication 30 November 2021; date of current version 12 September 2022. This work was supported in part by the Ministry of Science and ICT (MSIT), South Korea, through the Information Technology Research Center (ITRC) Support Program Supervised by the Institute for Information and Communications Technology Planning and Evaluation (IITP) under Grant IITP-2021-2018-0-01426 and in part by the Technology Innovation Program, Center for Composite Materials and Concurrent Design, funded by the Ministry of Trade, Industry and Energy (MOTIE), South Korea, under Grant 20013794. The Associate Editor for this article was S. A. Birrell. *(Corresponding authors: Kyuhyun Sim; Sung-Ho Hwang.)*

The authors are with the Department of Mechanical Engineering, Sungkyunkwan University, Suwon 16419, South Korea (e-mail: dodo1064@naver.com; hsh0818@skku.edu).

Digital Object Identifier 10.1109/TITS.2021.3128537

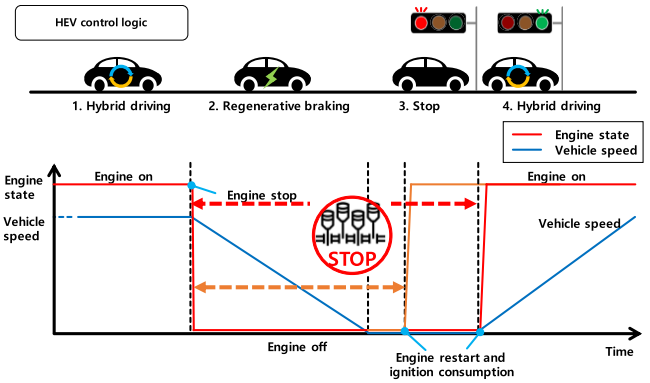

Fig. 1. The control logic of hybrid electric vehicles for when the vehicle stops.

algorithm through stop predictions. Section 5 analyzes the effectiveness of the control in transportation system using the traffic flow model. Section 6 concludes the paper.

II. A Control Algorithm of an Idle Stop and Go System With Traffic Signals

As mentioned before, if the traffic light turns green immediately after the engine has stopped, a short engine stop time may not have any benefit for improving fuel economy. A control algorithm is proposed to predict energy consumption when the vehicle is driving, decelerating, and starting. Figure 2 shows the flow chart for the control algorithm.

SAE J2735 [9] describes Signal Phase and Timing (SPAT), including the distance from the vehicle to the traffic light and the remaining time of the traffic signals. For example, when a traffic light turns red, the duration of the red light is transmitted. Also, the duration of the green light is known when the light turns green.

The algorithm acquires traffic signals and predicts when to stop. The next step is to confirm whether it is decelerating or not. The energy consumption is then calculated from the ICE BSFC (Brake Specific Fuel Consumption) map and the electric motor power map (Fig. 3). For example, when specific ICE rotational speed and torque are set in the dynamometer, the ICE consumes fuel, which is measured.

A new time value is defined. The fuel consumption is 0.6975 g when the ICE is cranking, extracted by a dynamometer test [10]. After cranking, the ICE is idling, and its idling fuel rate is 0.16 g/s. The cranking fuel consumption is divided by the idling fuel rate, which is 4.359 s according to equation (1). We defined the constraint time, t_{cst}. Energy consumption values are converted to time to utilize V2X data. The braking time is determined by taking into account the vehicle's braking performance.

$$t_{cst} = \frac{cranking\ fuel\ consumption}{idle\ fuel\ rate} \tag{1}$$

If the idle time is longer than the constraint time, properly turning the ICE off & on is more efficient than keeping the idle state. Conversely, if the idle time is shorter than the constraint time, keeping the ICE idle is more efficient than turning the ICE off & on.

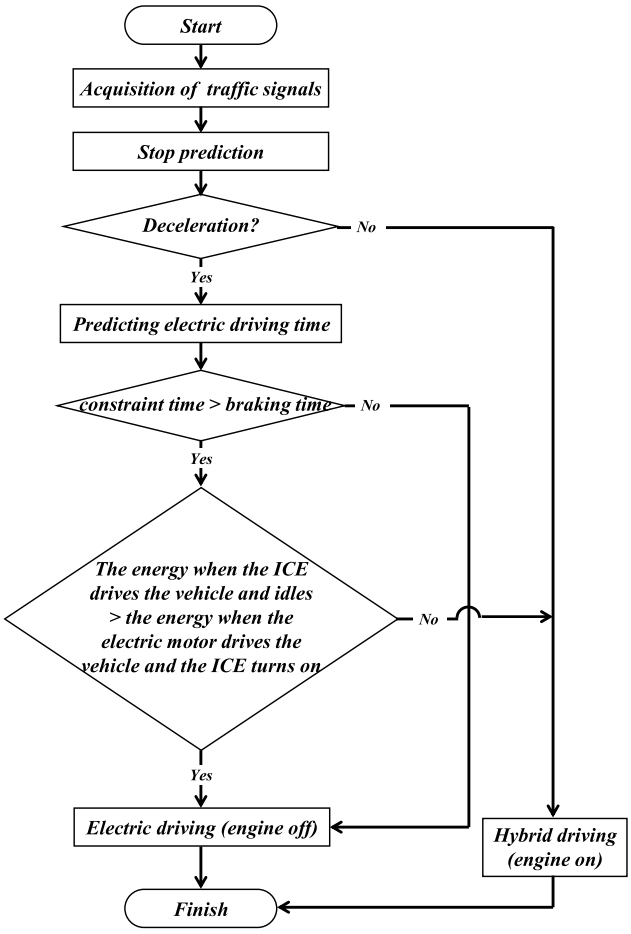

Fig. 2. The control algorithm of the extended idle stop and go system.

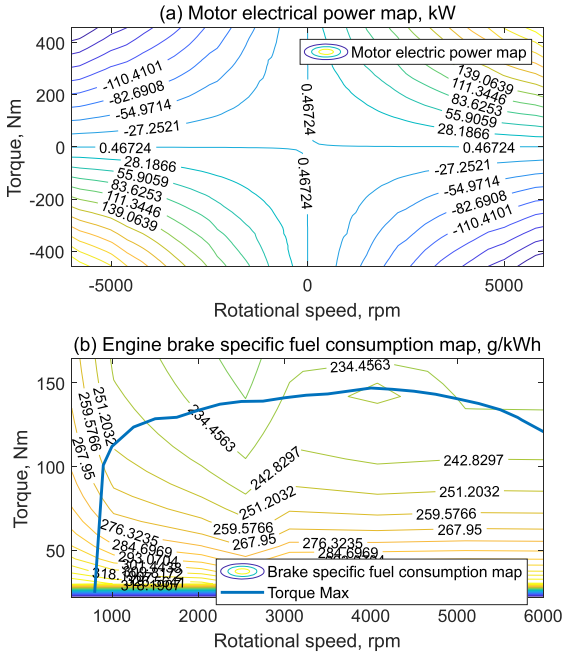

Fig. 3. Motor power and internal combustion engine (ICE) brake specific fuel consumption maps.

An HEV selects a more efficient driving mode by comparing the energy consumptions during EV and HEV driving modes. The EV mode is operating only an electric motor for driving. The HEV mode is operating both electric motor and ICE for driving. However, the EV mode needs the ICE idling when a battery is at a low state to charge. This case is that the ICE charges the battery to a specific high charge state without ICE propulsion.

The braking time is estimated using the current vehicle speed, the distance to the traffic light, and the braking performance. The vehicle stops, and the vehicle operation can be predicted during the stop time in front of the traffic light. The stop time is compared with the idling time to determine whether to keep the ICE idle or turn it off. However, the control can only be applied if the condition is satisfied.

HEVs can convert mechanical braking energy into electrical energy by an electric motor that provides regenerative energy. The controller keeps the battery SOC low before driving situations such as downhill deceleration, where much regenerative energy can be accumulated. If the acceleration/deceleration status of the vehicle is predicted through road information, the fuel economy of the vehicle can be increased by using this energy flow. The control algorithm selects a more efficient driving mode by comparing EV and HEV driving modes' energy consumption.

$E_{ondrvmot}$ and $E_{ondrveng}$ are the energy consumption when the electric motor operates and when the ICE operates, respectively, before decelerating. E_{stron} is the energy consumption when the ICE is turned on during cranking. E_{onbrk} is the energy consumption when the ICE is idle. Regenerative braking energy is not considered in this control because regenerative braking at deceleration is the same in EV and HEV driving modes. It assumes that the regenerative braking energy is regardless of any mode.

$$E_{ondrvmot} + E_{stron} < E_{ondrveng} + E_{onbrk} \tag{2}$$

If the above inequality is satisfied, the HEV driving mode is transferred to the EV driving mode when the electric motor drives the vehicle while the ICE turns off. The energy consumption at EV driving mode and the fuel consumption when the ICE drives the vehicle are calculated via the motor map and ICE map. The electrical energy is converted to fuel consumption using the equivalent conversion factor, F_{eq} [11].

$$E_{ondrvmot} = \int P(T_m, \omega_m) \times F_{eq} dt \tag{3}$$

$$E_{ondrveng} = \int fuelrate(T_e, \omega_e) dt \tag{4}$$

T_m and T_e are torques of the electric motor and ICE, respectively. ω_m and ω_e are rotational speeds of the electric motor and ICE, respectively. According to the motor efficiency, P is the motor power function of the motor torque and rotational speed, as shown in Fig. 3 (a). $fuelrate$ is the fuel rate function of the ICE torque and rotational speed from the engine BSFC map, as shown in Fig. 3 (b).

The fuel rate calculated when the ICE is idle can also be determined based on the ICE speed.

$$E_{onbrk} = fuelrate_{idling}(\omega_e) \times t_{vehstop} \tag{5}$$

TABLE I
TYPICAL STOPPING DISTANCES [12]

Vehicle speed	32 km/h	48 km/h	64 km/h	80 km/h	96 km/h	112 km/h
Recognizing distance	6 m	9 m	12 m	15 m	18 m	21 m
Braking distance	6 m	14 m	24 m	38 m	55 m	75 m
Stopping distance	12 m	23 m	36 m	53 m	73 m	96 m
Stopping time	2.025 s	2.775 s	3.375 s	4.095 s	4.800 s	5.496 s

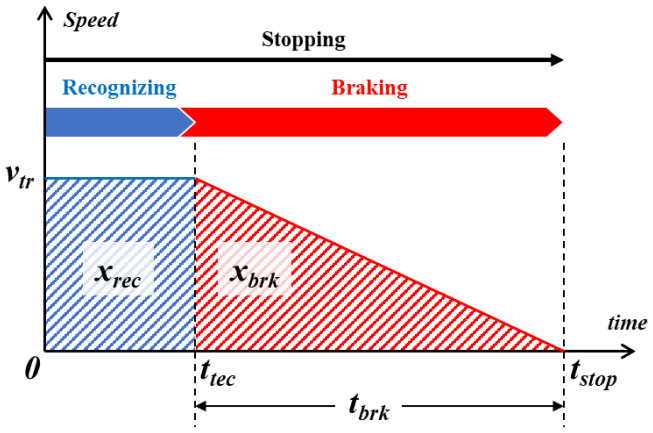

Fig. 4. A condition when the vehicle stops in front of traffic lights.

$fuelrate_{idling}$ is a fuel rate function of the ICE speed at idling. The energy consumption is estimated for the time, $t_{vehstop}$, when the vehicle stops at the traffic lights.

III. STOP PREDICTION ALGORITHM

The ISG control algorithm works only when a vehicle stops. Therefore, it is necessary to predict whether the vehicle stops. This paper determines whether the vehicle will stop by using the distance from the vehicle to the traffic light and the remaining time of the traffic signals.

The United Kingdom government proposed general rules, techniques, and advice for all drivers and riders. The stopping distances are among the guidelines, as shown in Table I [12]. The stopping times can be defined using distances and speeds. The recognizing distance is the driving distance over which a driver decides to stop while driving the vehicle. The braking distance is the driving distance traveled as the driver brakes the vehicle until the vehicle stops. The stopping time is the driving time for both the recognizing distance and braking distance. Figure 4 shows the condition when the vehicle stops in front of traffic lights. Suppose the vehicle travels at a constant speed during the recognizing distance and decelerates at a constant rate during the braking distance; as shown in Fig. 4, the stopping time can be calculated using the following equation.

$$t_{stop} = t_{rec} + t_{brk} = \frac{x_{rec} + 2x_{brk}}{v_{tr}} \tag{6}$$

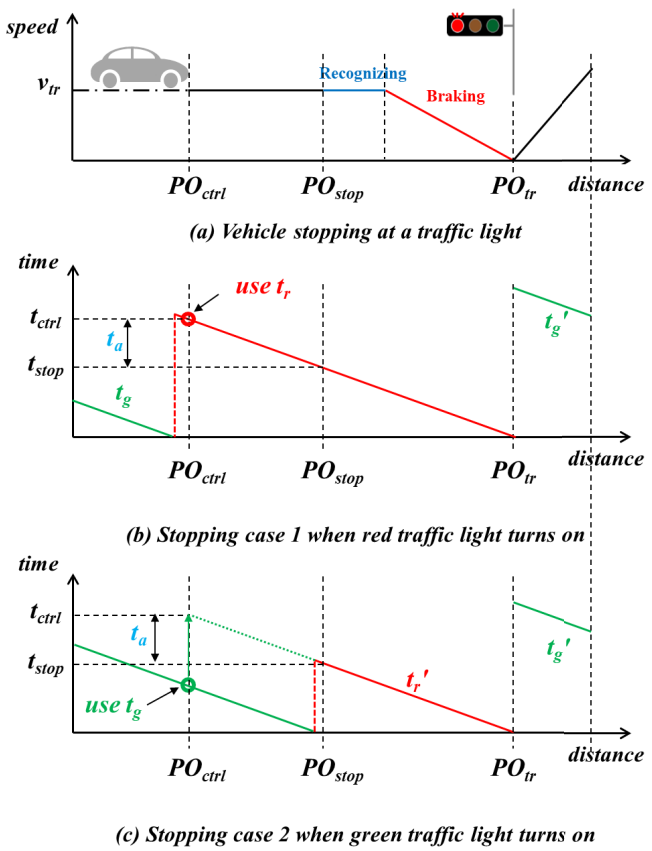

Fig. 5. (a) Vehicle speed when stopping according to distance, (b) stopping case 1 when a traffic light turns red, and (c) stopping case 2 when a traffic light turns green.

t_{stop}, t_{rec}, and t_{brk} are the stopping time, recognizing time, and braking time, respectively. x_{rec} and x_{brk} are the recognizing distance and braking distance, respectively. v_{tr} is the vehicle speed in front of traffic lights. It assumes that the braking time is constant depending on the vehicle speed.

The control point is PO_{ctrl} where the vehicle is driving a distance during the control time, t_{ctrl}, from the front traffic light, where the control algorithm determines which driving mode is more efficient, as shown in Fig. 5. It assumes that the control time is 5 seconds. Firstly, as the vehicle is at PO_{ctrl}, the traffic signal times and recognizing time are compared to predict whether the vehicle stops. The stopping possibility is proposed depending on the traffic signal time. The adjusting time is defined as t_a, which is the control time minus the stopping time.

$$t_a = t_{ctrl} - t_{stop} \tag{7}$$

If the remaining time of the red light, t_r, is less than the adjusting time, t_a, the vehicle does not stop and passes through the light. If t_r is greater than t_a, it can stop or pass through according to the possibility of passing. When t_r is closer to t_{ctrl}, the possibility of stopping increases. If t_r is greater than t_{ctrl}, the vehicle must stop at the traffic light.

On the contrary, if the remaining time of the green light, t_g, is less than t_a, it must stop. If t_g is greater than t_a, it may or may not pass through the light according to the possibility

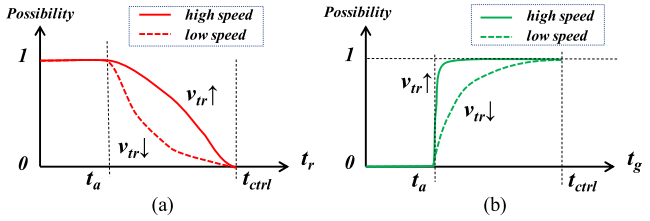

Fig. 6. Possibility of passing according to (a) red traffic signal and (b) green traffic signal.

of passing. When t_g is closer to t_{ctrl}, the possibility of passing increases. If t_g is greater than t_{ctrl}, the vehicle must pass the traffic light.

Two stopping cases are shown in Fig. 5. In Fig. 5 (b), the light turns red at PO_{ctrl} whereas the light turns green at PO_{ctrl} in Fig. 5 (c).

Figure 6 (a) shows the possibility of passing when a red light remains at the PO_{ctrl} point and Fig. 6 (b) shows the possibility of passing when a green light is at the PO_{ctrl} point. When the possibility is one, it passes through the front traffic light. When the possibility is zero, the vehicle stops in front of the traffic light. Depending on the vehicle speed, the possibility can change. High speed increases the possibility of passing, which represents the solid lines as shown in shown in Fig. 6. Conversely, low speed increases the possibility of stopping, which represents the dotted lines as shown Fig. 6. The high speed is 50 km/h, and the low speed is 30 km/h. As a result, the model can predict the stopping situation. When the stopping conditions are satisfied, the energy consumptions for each driving mode are calculated to decide which driving mode is more efficient using the proposed control. To obviously predict the stop situation, it assumes that the model predicted whether it is passing or stopping if t_g or t_r is lower than t_a and greater than t_{ctrl}.

The ISG time, t_{isg}, is time to decide whether to idle or not. The ISG time considers only the E_{stron} when the ICE is turned on during cranking and E_{onbrk} when the ICE is idle.

$$E_{stron} < E_{onbrk} \tag{8}$$

If the inequality (8) condition is satisfied, the engine sustains at idle state. However, the condition is limited, and the engine can turn on inefficiently. We propose the EV time, t_{EV}. It determines which the engine turns off and the motor provides forward propulsion under the condition that inequality (2) is satisfied. The t_{EV} is longer than the t_{isg}. The t_{EV} can increase the possibility in which the engine turns off before the vehicle brakes. When the deceleration condition is predicted, the driving modes are determined under given driving conditions for managing the HEV power more efficiently.

IV. Simulations of the Idle Stop and Go System

Using the developed backward simulator in Appendix A, the control algorithm is verified. The simulator calculates the energy consumptions. For the conventional ISG, case #1 in Fig. 7 is an example of when it is better to stop the ICE.

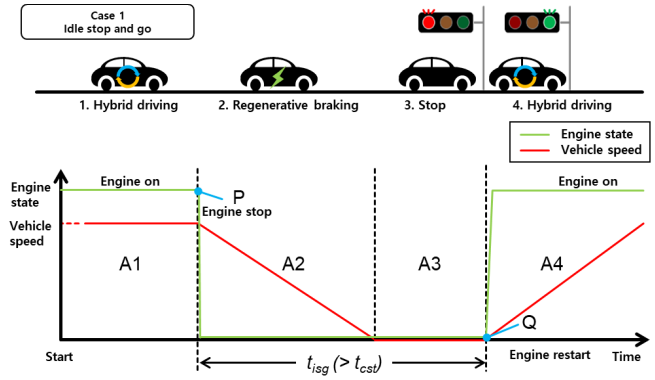

Fig. 7. Case 1: idle stop and go.

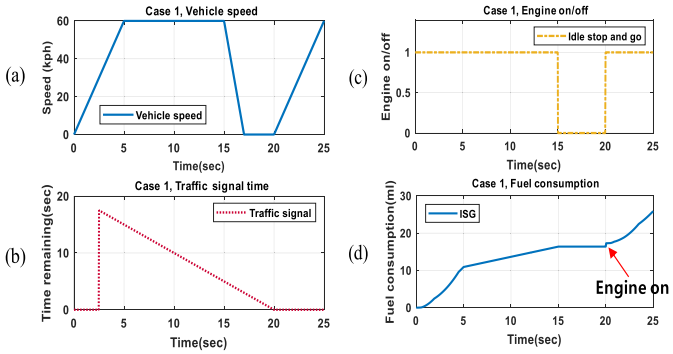

Fig. 8. Case 1 simulation results.

TABLE II

SUMMARY OF THE SIMULATION RESULTS FOR THE IDLE STOP AND GO CONTROL STRATEGIES

ISG time, t_{isg}	Constraint time, t_{cst}	Fuel consumption when the ICE is kept idle	Fuel consumption when the ICE restarts
5 s	4.359 s	26.04 ml	25.91 ml

Figures 8 (a) and (b) are the vehicle speed and traffic signal time conditions, respectively. When the ICE is kept idle, the fuel consumption is 26.04 ml. When the ICE turns off and restarts, the fuel consumption is 25.91 ml, demonstrating that turning off the ICE reduces the fuel consumption. Table II summarizes the results.

If t_{isg} is 5 seconds, greater than a t_{cst} of 4.359 seconds, the ICE turns off as shown in Fig. 8 (c), from 15 to 20 seconds. At 20 seconds, the ICE turns on and its fuel consumption increases, as shown in Fig. 8 (d),

$$t_{isg} > t_{cst}. \tag{9}$$

Case 2-1 and 2-2 are examples where it is better to keep the ICE idling. The driving conditions of 2-1 and 2-2 are the same they produce different results depending on the control algorithm, as shown in Figs. 9 and 10, respectively. Figures 11 (a) and (b) show the vehicle speed and traffic signal time conditions, respectively. In case 2-1, the ICE is kept idling by the basic control shown in Fig. 11 (c). However, in the case of 2-2, an extended ISG control turns off the ICE

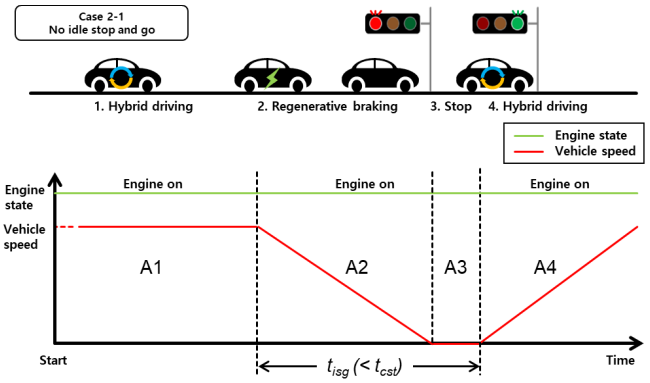

Fig. 9. Case 2-1: no idle stop and go.

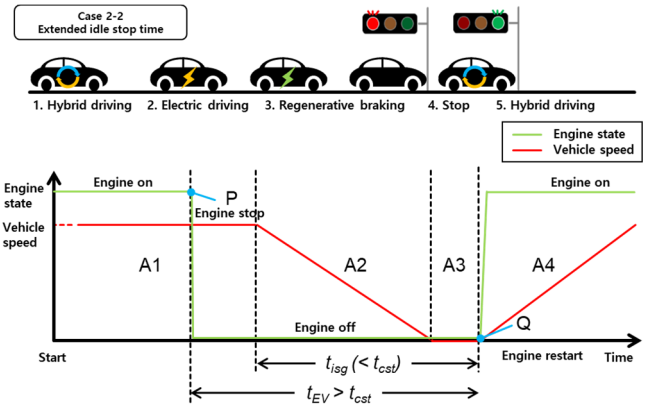

Fig. 10. Case 2-2: an extended engine-off time.

TABLE III

SUMMARY OF THE SIMULATION RESULTS FOR THE IDLE STOP AND GO (ISG) CONTROL STRATEGIES

Proposed EV time, t_{EV}	ISG time, t_{isg}	Constraint time, t_{cst}	Fuel consumption of ISG	Fuel consumption of the extended ISG	Improvement
5.0 s	4 s	4.359 s	28.68 ml	28.39 ml	1.04 %
5.5 s	4 s	4.359 s	28.68 ml	28.21 ml	1.64 %
6.0 s	4 s	4.359 s	28.68 ml	28.02 ml	2.31 %

in which the value of t_{EV} is newly defined and it is more efficient to turn the ICE on and off, as shown in Figure 11 (d). Table III summarizes the results. Because the t_{isg} is less than the constraint time, t_{cst}, it is better to keep the ICE idling. However, if t_{EV} is more than t_{cst}, the energy consumptions of the controls should be compared. If it is better to operate in the EV driving mode while the ICE turns off before braking, the ICE idling stops.

$$t_{EV} > t_{cst} > t_{isg} \tag{10}$$

Figure 12 shows the different fuel consumptions in the controls. The extended ISG operates an electric motor and the ICE in HEV driving after 13 seconds, as shown in Fig. 12 (b).

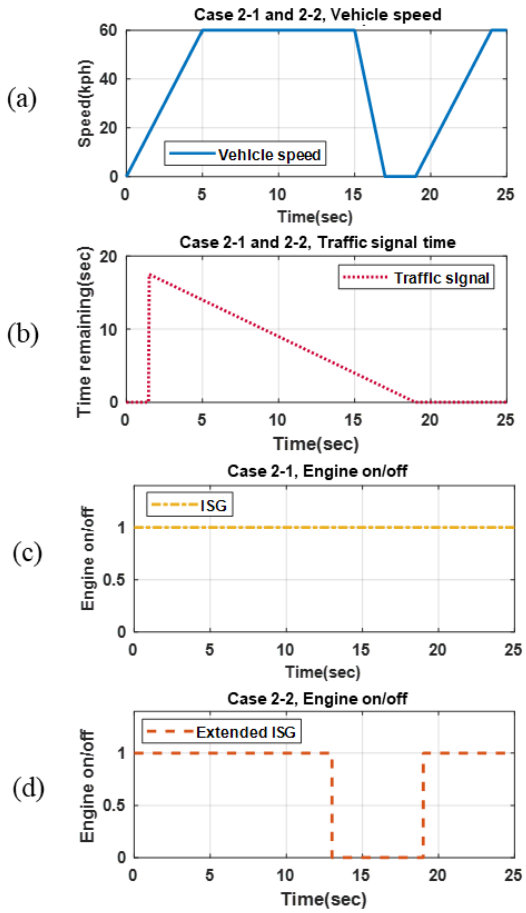

Fig. 11. Case 2 simulation results: (a) vehicle speed, (b) traffic signal time, (c) engine on/off signal in the basic idle stop and go (ISG) control, and (d) engine on/off signal in the extended ISG control.

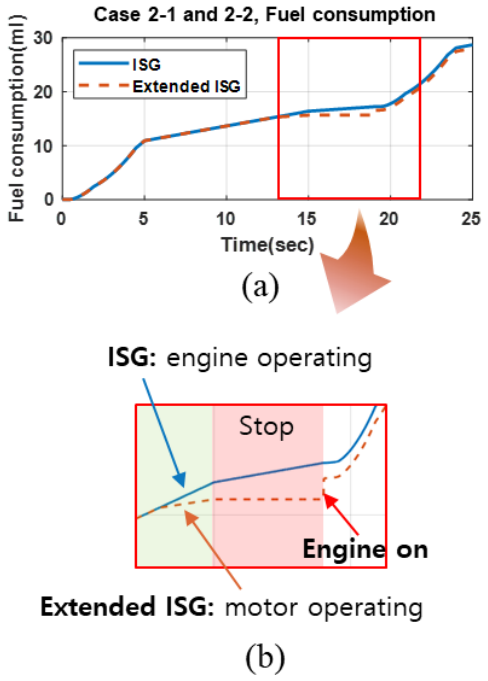

Fig. 12. Case 2-1 and 2-2 simulation results: fuel consumption in (a) a basic idle stop and go (ISG) control, and (b) an extended ISG control.

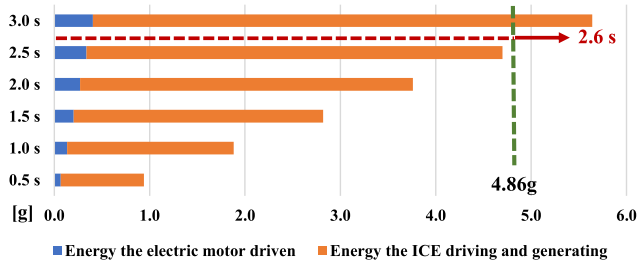

Fig. 13. A constraint time that benefits from driving with an electric motor and later when the ICE generates electrical energy.

When the ICE restarts, the fuel of the ICE ignition is consumed.

In the case of defining t_{EV} as 5 seconds which is higher than t_{isg} by 1 second, 28.68 ml of fuel is consumed in the basic control. However, the proposed control consumes 28.39 ml of fuel, resulting in a reduction of 1.04%. Additionally, if t_{EV} is defined as 6 seconds which is higher than t_{stop} by 2 seconds, the proposed control consumes 28.02 ml of fuel, resulting in a reduction of 2.31%.

Increasing t_{EV} consumes more electrical power and it can deteriorate powertrain efficiency because the electrical energy consumed must be charged by the ICE generating power to convert the fuel to electrical energy. However, this energy circulation can be eliminated by regenerating the braking energy that otherwise would have been lost. If the EV driving mode is used instead of the HEV driving mode, the equivalent fuel consumed is 0.27 g, which is equivalent to the electrical energy for 2 seconds. Additionally, if the energy is calculated that the ICE generates electrical energy for the consumed electrical energy, 3.49g is required for 2 seconds. The sum of the two equivalent fuels obtained previously must be less than the energy obtained during regenerative braking. The fuel amount by regenerative braking is 4.86 g, which is equivalent to electric energy. Therefore, it is advantageous to drive from HEV mode to EV mode when it is at least 2.6 seconds as shown in Fig. 13. Restarting the ICE after EV driving rather than keeping the ICE idling in the HEV driving mode helps to reduce fuel consumption. Three fuel consumptions are obtained by calculating electrical energies at each time, with the equivalent conversion factor as used in the calculation of energy consumption.

Using the driver-in-the-loop simulation in Appendix B, the stop prediction developed was validated.

For virtual driving conditions, traffic lights are located at equidistant distances on a straight road with limited speeds. There are surrounding vehicles that follow the UDDS cycle. When the vehicles stop according to the red traffic signal, they stop following the cycle. When the signal turns green, the vehicles continue the cycle. The developed PHEV is driven by a driver under virtual driving conditions. Cases 1 and 2 show the results of driving at 50 km/h. Figure 14 shows the traffic conditions. Figures 15 and 16 show the case 1 and case 2 results, respectively. Two cases are attempts of the

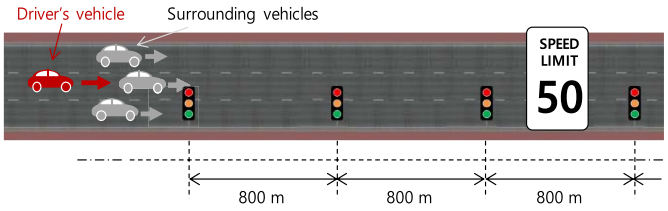

Fig. 14. Simulation traffic conditions of traffic lights position and surrounding vehicles.

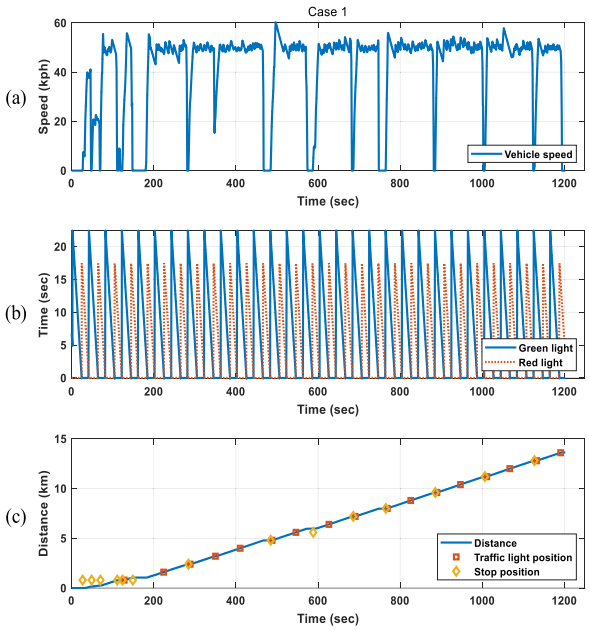

Fig. 15. Case 1 simulation results of the (a) vehicle speed, (b) traffic signal times, and (c) vehicle distance, traffic light positions and vehicle stop positions.

driver driving in the same test scenario where the driver cruises at 50 km/h, and the surrounding vehicle and traffic signals are the same. However, because the driver's behaviors in the two cases are subtly different, the situations encountered are different, affecting the simulation results.

In case 1, the distance traveled is 13.6 km, and the vehicle goes through 17 traffic lights. Among them, the number of traffic lights stopped at is 9. With the stop prediction algorithm, the number of predicted stops is nine, and the stop prediction probability is 100%. Table IV summarizes the case 1 results, including the traffic signal times and stop prediction probability.

In case 2, the distance traveled is 9.7 km, and the vehicle goes through 12 traffic lights. Among them, the number of traffic signals stopped at is 6. With the stop prediction algorithm, the number of predicted stops is 4, and the prediction success probability is 66.7%. The reason for these two failures is that the vehicle speed is different from the given speed of 50 km/h at the predicting time. The vehicle could not accelerate to 50 km/h because of the surrounding vehicles. These vehicles affect the prediction. In the next study, the limitation needs to be solved. Table V summarizes the case 2 results of the traffic signal times and the stop prediction probability.

TABLE IV

CASE 1 TRAFFIC SIGNAL TIMES, STOP RESULT, AND STOP PREDICTION AT TRAFFIC LIGHT POSITIONS

Number of traffic light	Green signal time, t_g	Red signal time, t_r	Simula-tion results	Predict-ed	Stop prediction
1	0	15.41	Stop	Stop	Success
2	6.21	0	Pass	Pass	-
3	0	5.61	Stop	Stop	Success
4	2.51	0	Pass	Stop	-
5	20.42	0	Pass	Pass	-
6	3.13	0	Stop	Stop	Success
7	4.86	0	Stop	Stop	Success
8	4.91	0	Pass	Stop	-
9	0	5.51	Stop	Stop	Success
10	2.49	0	Stop	Stop	Success
11	6.21	0	Pass	Pass	-
12	0	6.61	Stop	Stop	Success
13	5.41	0	Pass	Stop	-
14	0	6.27	Stop	Stop	Success
15	5.64	0	Pass	Stop	-
16	0	5.20	Stop	Stop	Success
17	2.11	0	Pass	Stop	-

TABLE V

CASE 2 TRAFFIC SIGNAL TIMES, STOP RESULT, AND STOP PREDICTION AT TRAFFIC LIGHT POSITIONS

Number of traffic light	Green signal time, t_g	Red signal time, t_r	Simula-tion results	Predict-ed	Stop prediction
1	0	11.31	Stop	Stop	Success
2	4.61	0	Pass	Stop	-
3	0	5.13	Stop	Stop	Success
4	4.03	0	Pass	Stop	-
5	0	3.58	Pass	Stop	-
6	7.78	0	Pass	Pass	-
7	0	7.92	Stop	Stop	Success
8	14.65	0	Stop	Pass	Failure
9	6.65	0	Stop	Pass	Failure
10	21.73	0	Pass	Pass	-
11	0	8.26	Stop	Stop	Success
12	16.07	0	Pass	Pass	-

This simulation is applied using the backward simulation results. If the stop prediction is 100%, the average fuel consumption reduction is 2.47% for cases 1 and 2. With the stop prediction algorithm and the proposed ISG control system, the reduction is 2.12%. The stop prediction algorithm is improved, higher energy efficiency improvement will be possible.

V. ANALYSIS OF TRANSPORTATION SYSTEM WITH A TRAFFIC FLOW MODEL

In terms of the transportation system, how the proposed control algorithm improves energy efficiency is validated in

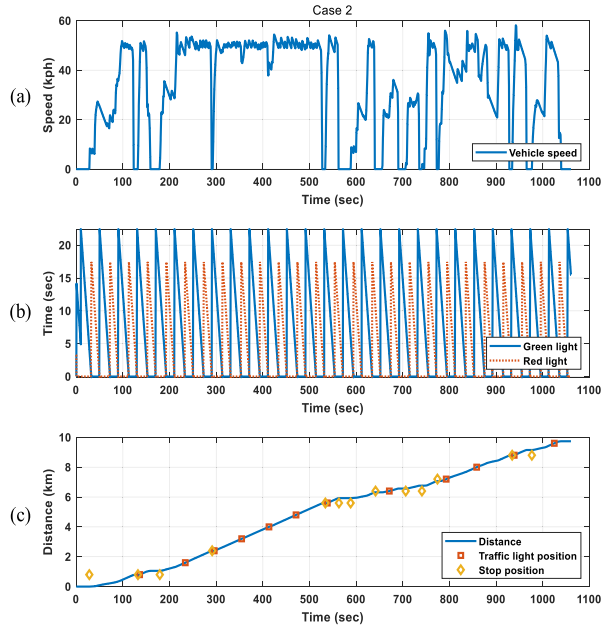

Fig. 16. Case 2 simulation results of the (a) vehicle speed, (b) traffic signal times, and (c) vehicle distance, traffic light positions and vehicle stop positions.

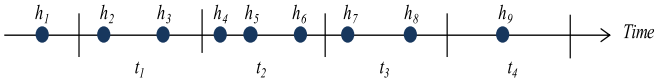

Fig. 17. A traffic flow model [21].

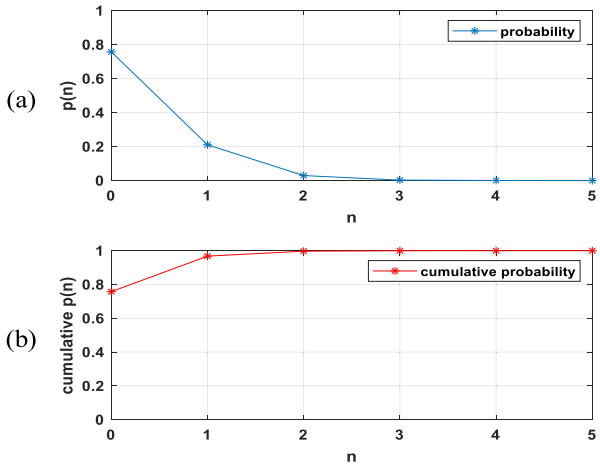

Fig. 18. The (a) probability and (b) cumulative probability of the Poisson distribution for a traffic flow model.

this section. The traffic flow model uses a Poisson distribution, which is probability of exacting the number of vehicles arriving in a time interval [13]. Figure 17 shows that h represents the vehicle headway in a time interval t. The equation for the Poisson distribution [14] is

$$p(n) = \frac{m^n e^{-m}}{n!}, \tag{11}$$

where p is the probability, m is the average number of vehicles in a time interval, n is the number of vehicles arriving in a time interval, and e is the base of the natural logarithm. The equation for the cumulative probability is

$$p(n \leq) = \sum_{k=0}^{q} p(k), \tag{12}$$

where q is a number and k is an arbitrary number.

The driving conditions assume that the traffic lights are equidistant from a straight road of 800 m, and the vehicle runs at an average speed of 50 km/h, the same conditions used in the previous simulation. Figure 18 shows the Poisson distribution, which is the probability that vehicles exist in the red signal time interval. The probability is calculated based on the number of vehicles. Figures 18 (a) and (b) show the probability and cumulative probability, respectively.

If the vehicle does not arrive within the time interval, the probability is 0.758. Conversely, the probability is 24.2% if there exists at least one vehicle in the red signal time interval. If the vehicle drives on a 12 km long straight road and there are 15 traffic lights at equal intervals of 800 m, the 3.64 traffic lights turn red based on the probability. When the vehicle stops three times in front of the red light, the proposed ISG control system reduces the energy consumption by 1.05%.

The Annual Energy Outlook 2019 estimated transportation energy use for light-duty vehicles by the powertrain type [15]. Compared to 2017, total vehicle sales growths are 0.5% and 6.4% in 2035 and 2050, respectively. Above all, EVs and HEVs are increasing due to the advancement of vehicle electrification technology. In 2035 and 2050, sales of electric hybrids and plug-in electric hybrids increases by 126% and 171%, respectively. Table VI summarizes the energy use of the HEVs, which include an electric-gasoline hybrid, plug-in 40 gasoline hybrid, and plug-in ten gasoline hybrid. The electric-gasoline hybrid is charge-sustaining. The plug-in 40 gasoline hybrid and plug-in ten gasoline hybrid have 40 miles and 10 miles electric ranges, respectively. The proposed ISG control system will apply to almost all HEVs. The plug-in hybrid can also be driven like a conventional HEV when all the electric energy is consumed. If the control system reduces energy use by 9.5% according to the above efficiency improvement of 1.05%, it will reduce the HEV energy use. In 2020, the energy use can be reduced by 6.685tWh (trillion Watt hour). This reduction value is more than those of the plug-in 40 gasoline hybrid or the plug-in ten gasoline hybrid. In addition, the reduction accounts for 1.9 times the annual energy generation of Korea's 400MW Cheongpyeong pumped-storage hydroelectric power plant. The value is also equivalent to 90% of the annual energy generation of the Yeongwol combined cycle power plant in Korea, which is 848.055 MW.

In 2035 and 2050, the energy use can be reduced by 12.485 and 17.933tWh, respectively. The reductions are more than half of the plug-in 40 gasoline hybrid or plug-in ten gasoline hybrid. Though the energy efficiency improvement reduces the energy use, the vehicle electrification and HEV market growth will gradually increase their energy uses, according to estimated values. When all vehicles are connected cars

TABLE VI
TRANSPORTATION ENERGY USE ESTIMATION AND THE EFFECTIVENESS OF THE PROPOSED ISG CONTROL SYSTEM (UNIT: TRILLION WATT HOUR, tWh) [15]

Year	2020	2035	2050
1. Hybrid electric vehicles energy use without the proposed control	70.343	131.393	188.717
1.1 Electric-gasoline hybrid	60.135	93.047	129.728
1.2 Plug-in 40 gasoline hybrid	5.255	18.182	29.026
1.3 Plug-in 10 gasoline hybrid	4.950	20.163	29.967
2. Hybrid electric vehicles energy use with the proposed control	63.658	118.908	170.787
3. Energy use reduction due to the proposed control	6.685	12.485	17.933

equipped with V2X technology and stop prediction is realized, the proposed technique will improve HEV energy efficiency and reduce energy use.

VI. CONCLUSION

This paper proposed a control algorithm of an idle stop and go (ISG) system and a stop prediction algorithm. The basic ISG system was limited to certain conditions, and then, a new braking time is proposed for a hybrid electric vehicle to improve the ISG and reduce fuel consumption. In comparing energy consumptions, the control algorithm determines when to turn off an internal combustion engine (ICE). If the ICE turns off and an electric motor operates the vehicle at a stopping point, it can reduce fuel consumption with regenerative braking energy. However, the control algorithm is effective only if the stop condition is known. A stop prediction algorithm predicts whether a vehicle will stop at traffic lights, using braking performance and traffic signal time information. The traffic signal information and driving simulation results were obtained with the driver-in-the-loop simulator, and the stop prediction algorithm was validated. The proposed ISG with the stop prediction can reduce fuel consumption by 2.12%.

The traffic flow model calculated the probability of a vehicle arriving in a red signal time interval using a Poisson distribution. According to the traffic flow model, the proposed ISG was evaluated and validated to improve the vehicle's energy efficiency in the various traffic situation.

APPENDIX A
PERFORMANCE SIMULATORS FOR AN IDLE STOP AND GO SYSTEM

A performance simulator was developed to verify the ISG system and control algorithm [16]. Figure 19 (a) shows a forward simulator of an HEV with a pre-transmission parallel hybrid structure in which the vehicle system consists of an ICE, electric motor, hybrid starter generator (HSG), engine clutch, transmission, and battery. The HEV's performance simulator was developed using MATLAB/Simulink based on system dynamics and experimental data. Table VII shows the parameters of the PHEV components. All component models

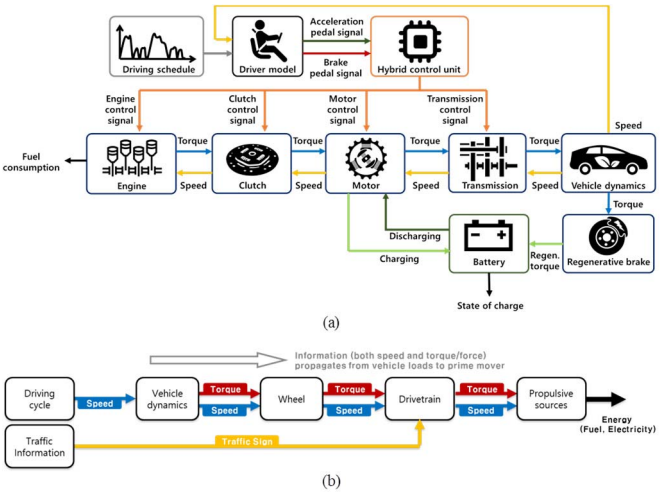

Fig. 19. Concepts of (a) a forward simulator and (b) a backward simulator.

TABLE VII
VEHICLE SPECIFICATION

Components	Parameters	Values
Vehicle	Mass	1,321 kg
Internal combustion engine	Displacement / maximum power	1.6 L / 77 kW
Electric motor	Maximum power	32 kW
Dual clutch transmission	Gearbox	6-speed
Battery	Capacity	1.56 kWh

are quasi-static. The correlation process with the actual system was performed to verify the models including the battery state of charge and the powertrain models. Also, a backward simulator was developed. Given the driving cycle and traffic information, energy consumption is calculated using the vehicle dynamics and powertrain model as shown in Fig. 19 (b). The vehicle model is based on the same model as in the forward simulator.

APPENDIX B
A DRIVER-IN-THE-LOOP SIMULATOR WITH TRAFFIC CONDITIONS

A vehicle powertrain model calculates energy consumption and virtual driving simulation controls traffic signals. A driver-in-the-loop simulator was developed for a driver to drive a vehicle in virtual driving environment according to traffic conditions. The electric motor and internal combustion engine of the vehicle can calculate the energy consumption while the vehicle is running.

The driver-in-the-loop simulator consists of a virtual driving environment model and a real-time target model of PHEV [17]. Figure 20 shows a diagram of the driver-in-the-loop simulation. A host computer visualizes the virtual driving environment, debug panel, and initializing panel in real time. It also saves the simulation data. It shows virtual driving environments developed by 3D physics modeling. A real-time computer, National Instruments (NI) compact RIO

TABLE VIII
DRIVING PATTERN FACTORS FOR THE DRIVER-IN-THE-LOOP SIMULATIONS

Driving Cycle	UDDS	Cruise	Case 1	Case 2
Average speed	38.85 km/h	68.20 km/h	44.93 km/h	38.63 km/h
Average acceleration	0.505 m/s^2	0.077 m/s^2	0.028 m/s^2	0.033 m/s^2
Average deceleration	-0.578 m/s^2	-0.082 m/s^2	-0.015 m/s^2	-0.016 m/s^2
Standard deviation of the acceleration	0.451 m/s^2	0.088 m/s^2	0.076 m/s^2	0.075 m/s^2
Maximum speed	91.25 km/h	95.05 km/h	60.30 km/h	58.17 km/h
Maximum acceleration	1.475 m/s^2	0.420 m/s^2	0.559 m/s^2	0.525 m/s^2
Maximum deceleration	-1475 m/s^2	-0.595 m/s^2	-1.948 m/s^2	-1.426 m/s^2
Relative positive acceleration	0.165 m/s^2	0.028 m/s^2	0.201 m/s^2	0.238 m/s^2
% of time when $v < 2$ km/h	20.45%	8.16%	12.51%	17.06%
Frequency of oscillation of the speed curve per 100 s	7.82	4.46	27.79	25.94

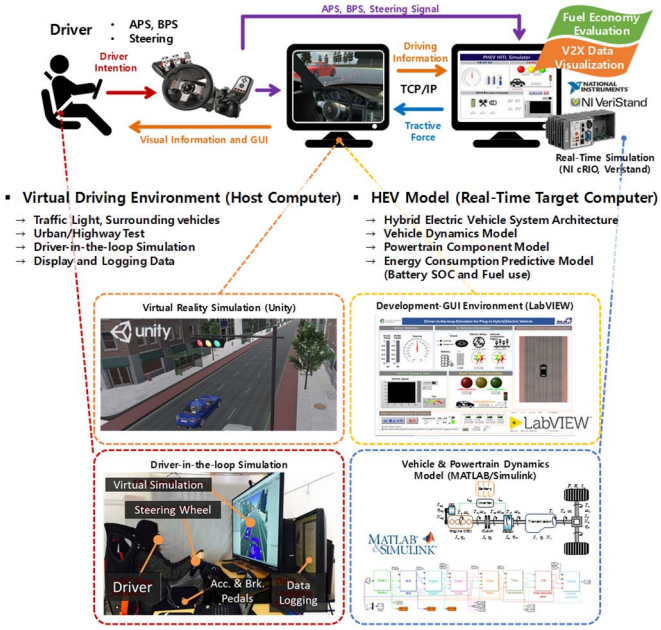

Fig. 20. A diagram of the driver-in-the-loop simulator.

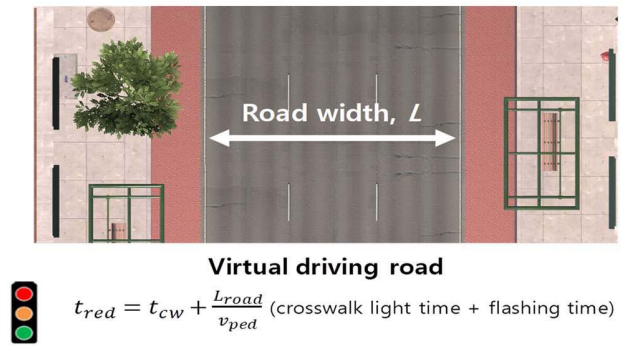

Fig. 21. A diagram of the driver-in-the-loop simulator.

(1.33 GHz Dual-Core, RAM 1GB), simulates in NI Veristand, which helps the hardware-in-the-loop simulation. This simulation includes the developed forward simulator based on MATLAB/Simulink. Vehicle controller can be developed and imported into the vehicle model. The host and real-time computers are connected with TCP/IP.

When a driver controls the acceleration and brake pedals as well as the steering wheel, the virtual driving environment visualizes vehicle motions and the surrounding traffic environment [18]. Acceleration and brake pedal signals are sent to the real-time model. The display and control panel shows the driver intentions (acceleration and brake pedals, steering angle), powertrain data (hybrid clutch state, motor and engine speeds, and battery state), vehicle dynamics (longitudinal speed and yaw), traffic signals (signal remanding time), surrounding vehicles (relative position to driving vehicle), data communication information, and the simulation controller.

When a driving cycle, which is the vehicle speed versus time profile, has to be given *a priori* in most simulators [19], the driver operates the vehicle model directly and the driving cycle is generated simultaneously by a driving simulation. The driving environment includes traffic signals and surrounding vehicles in urban and highway tests. The driving actuators are acceleration and brake pedals, as well as the steering wheel. Lateral vehicle dynamics are contained in the virtual driving environment model. The real-time model has longitudinal vehicle dynamics and an energy consumption predictive model, which is the forward simulator modified for real-time simulation. The sampling time for the real-time simulation is 1 ms and the time interval for logging is 10 ms. The simulation is realized in real-time.

The virtual vehicle drives straight on a three-lane road. The surrounding driving environments, including buildings and trees, exist only around the vehicle. The environments which the vehicle passes disappear and new environments are created around the moving vehicle. In addition, if the vehicle travels more than a certain distance, the vehicle is relocated back to the starting point. Hence, a driver feels like they are driving on an infinite road due to this environment.

The traffic lights are set by a document of the transportation operating system [20]. Figure 21 shows the top-view of the virtual driving road and pedestrian crossing signal. The green pedestrian signal time when a vehicle stops is determined by the sum of the initial additional time and pedestrian flashing time. The flashing time is the pedestrian passing distance

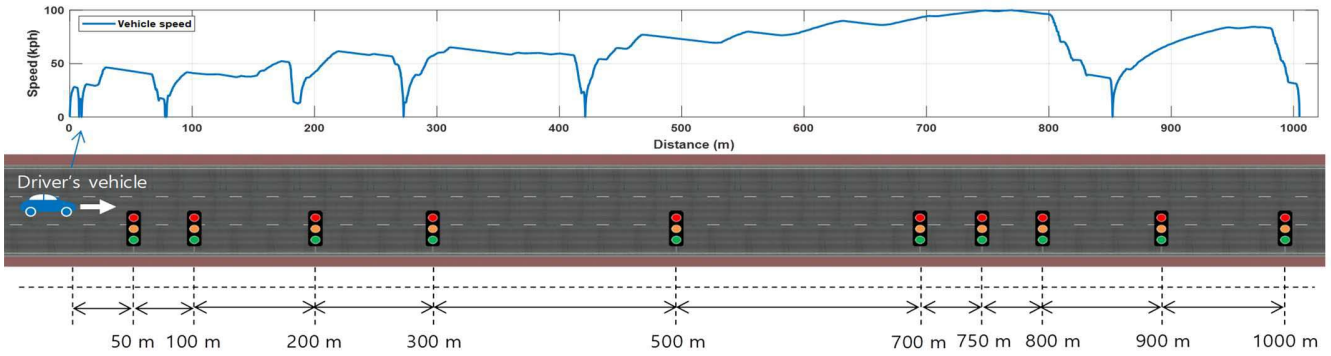

Fig. 22. Simulation vehicle speed and traffic conditions.

divided by the pedestrian walking speed.

$$t_r = t_{cw} + L_{road}/v_{ped} \tag{13}$$

t_r is duration of the red phase of the traffic lights. t_{cw} is duration of the crosswalk warning light. L_{road} is road width and v_{ped} is the pedestrian walking speed.

The signal time is 17.5 s and the vehicle stops as long as the time remains.

A virtual reality driving simulator needs to evaluate how strongly a driver experiences presence in the simulator without sickness [21]. For simulator evaluation, there are a presence questionnaire [22] and a simulator sickness questionnaire [23]. Although a discrepancy between the virtual environment and real-life driving is important, the developed simulator focuses on vehicle performance, not on the driver's feeling. The two questionnaires were not considered in this research. The developed simulator evaluates energy efficiency and PHEV performance. Because it uses the same powertrain model of the forward simulator, its powertrain efficiency and mode transition are the same as those of the forward simulator. In addition, the vehicle accelerating, and braking performances are also the same as a real target vehicle. Using the forward simulator, acceleration and deceleration tests were conducted before the vehicle model was applied to the driver-in-the-loop simulator. When the acceleration pedal signal and braking pedal signal are at their maximum values, the vehicle performance was validated by comparing it to that of the target vehicle.

Figure 22 shows the traffic conditions and the vehicle speed results. The road is straight and contains 10 traffic lights, as shown in Fig. 22. Figure 23 shows the simulation results. When a driver commands the acceleration pedal signal (APS) and brake pedal signal (BPS), the vehicle speeds up and down, as shown in Figs. 23 (a) and (b). As the control algorithm of the HCU, the driving modes were changed from the electric driving mode to the hybrid driving mode or vice versa, as shown in Fig. 23 (c). The gear state also changes based on the transmission shift map as shown in Fig. 23 (d). The battery state of charge (SOC) was depleted, as shown in Fig. 23 (e). The energy efficiency was 21.3 km/l, which was calculated simultaneously as shown in Fig. 23 (f). The traffic signal remaining times are shown in Fig. 23 (g). The green light and red light remaining times were known. Finally, when the vehicle stopped, its distances were sustained and the

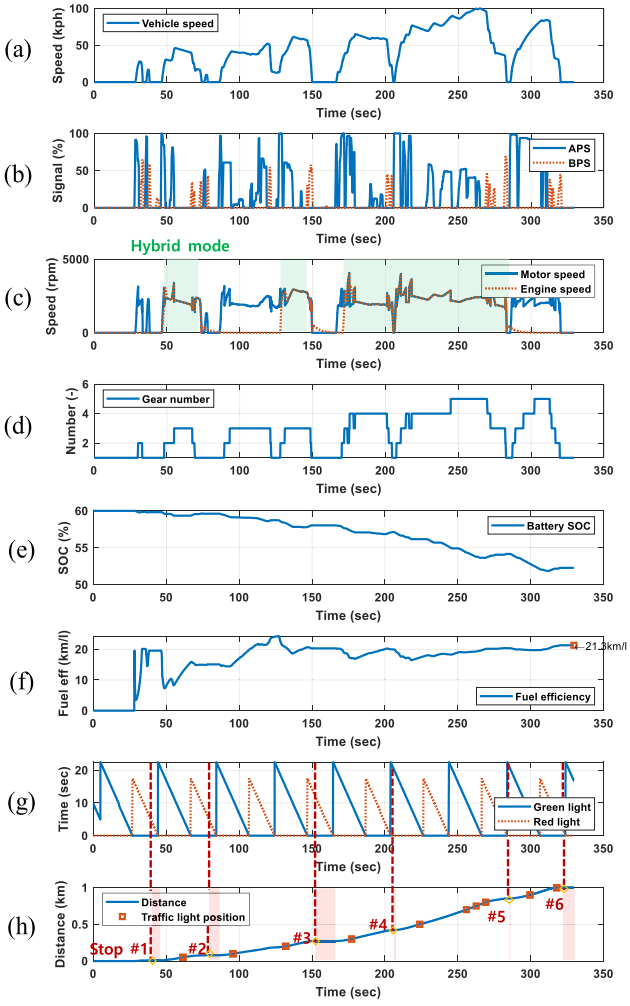

Fig. 23. Driver-in-the-loop simulation results: (a) vehicle speed, (b) acceleration and brake pedal signals, (c) motor and engine speed, (d) gear state, (e) battery state of charge, (f) energy efficiency, (g) traffic signal remaining times, and (h) vehicle driving distance with traffic light positions.

light turned red. When a light changed from red to green, the vehicle did not start right away, as shown in Fig. 23 (h).

APPENDIX C
DRIVING PATTERN FACTORS

This appendix is to analyze the vehicle speed profile the driver-in-the-loop simulations in section 4. A vehicle speed profile is a simulation result of the vehicle speed in

time domain. Figure 23 (a) is an example of vehicle speed profile. The analysis method uses driving pattern factors [24]. There are several ways to analyze the relationship between fuel economy-related factors [25]. For example, regression analysis, neural network, etc. Here, correlation analysis and regression analysis were used. The driving pattern factors consist of average and maximum speed, acceleration, and deceleration, and so on. Table VIII shows the driving pattern factors for UDDS, cruise, and two case cycles. They were a part of the driving pattern factors reported previously. Two case cycles have characteristics of the UDDS and cruise cycles. According to the two case cycles, the average acceleration, average deceleration, standard deviation of the acceleration, and maximum acceleration are similar to those of the cruise cycle. Additionally, the maximum deceleration, relative positive acceleration, and the percentage of time when the vehicle speed is lower than 2 km/h are similar to those of the UDDS cycle. Because traffic lights are located at equidistant distances on a straight road by cruising at 50 km/h, the two case cycles represent cruise driving in a city.

REFERENCES

[1] J. Wichart and M. Shirk, "Quantifying the effects of idle-stop systems on fuel economy in light-duty passenger vehicles," Idaho Nat. Lab., Falls, ID, USA, Tech. Rep. INL/EXT-12-27320, Dec. 2012.

[2] G.-M. Hwang, Y.-T. Kwon, S.-S. Ko, and J.-K. Choi, "A reaserch on fuel economy improvement by intelligent idle stop & go," *Trans. Korean SoC. Automot. Eng.*, vol. 22, no. 1, pp. 71–76, Jan. 2014.

[3] C. Sun, X. Shen, and S. Moura, "Robust optimal ECO-driving control with uncertain traffic signal timing," in *Proc. Annu. Amer. Control Conf. (ACC)*, Milwaukee, WI, USA, Jun. 2018, pp. 5548–5553.

[4] N. Kim, D. Karbowski, and A. Rousseau, "A modeling framework for connectivity and automation co-simulation," SAE, Warrendale, PA, USA, Tech. Rep. 2018-01-0607, 2018.

[5] U.S. Department of Transportation. *Connected Vehicles—CV Piot Depoyment Program*. Accessed: Dec. 9, 2018. [Online]. Available: https://www.its.dot.gov/pilots/cv_pilot_apps.htm

[6] European Center for Information and Communication Technologies. *DRIVE C2X*. Accessed: Dec. 16, 2018. [Online]. Available: https://www.eict.de/projekte/#project-8

[7] B. Y. Kong, "Control method for idle go/stop," Korean Patent 0 057 452, Jun. 14, 2011.

[8] S. H. Hwang, C. H. Park, K. Sim, and S. M. Oh, "Method for controlling the engine of a hybrid vehicle," Korean Patent 1 738 818, May 16, 2017.

[9] *Dedicated Short Range Communications (DSRC) Message Set Dictionary*, SAE International, Detroit, MI, USA, 2016.

[10] S. Choi, S. Choi, and M. H. Son, "The effect of engine idling stop for vehicle fuel economy," in *Proc. Korean Soc. Automot. Eng. Daejeon Chungcheong Spring Conf.*, Seoul, South Korea, 2009, pp. 64–65.

[11] A. Khajepour, M. Fallah, and A. Goodarzi, *Electric and Hybrid Vehicles: Technologies, Modeling and Control—A Mechatronic Approach*. Hoboken, NJ, USA: Wiley, 2014.

[12] United Kingdom Government Department for Transport. *The Highway Code: General Rules Techniques and Advice for All Drivers and Riders*. Accessed: May 7, 2019. [Online]. Available: https://www.gov.U.K./guidance/the-highway-code/general-rules-techniques-and-advice-for-all-drivers-and-riders-103-to-158

[13] T. V. Mathew, *Transportation Systems Engineering Chapter 13: Vehicle Arrival Models L Count*. Chennai, India: NPTEL. Accessed: Jun. 10, 2019. [Online]. Available: https://nptel.ac.in/downloads/105101008/

[14] A. D. May, *Traffic Flow Fundamentals*. Upper Saddle River, NJ, USA: Prentice-Hall, 1990.

[15] U.S. Energy Information Administration. *Annual Energy Outlook 2019, Table: Light-Duty Vehicle Energy Consumption by Technology Type and Fuel Type*. Accessed: Jun. 10, 2019. [Online]. Available: https://www.eia.gov/outlooks/aeo/data/browser/#/?id=47-AEO2019&region=0-0&cases=ref2019&start=2017&end=2050&f=A&linechart=&map=&sourcekey=0

[16] K. Sim, S. M. Oh, C. Namkoong, J. S. Lee, K. S. Han, and S. H. Hwang, "Control strategy for clutch engagement during mode change of plug-in hybrid electric vehicle," *Int. J. Automot. Technol.*, vol. 18, no. 5, pp. 901–909, 2017.

[17] S. H. Hwang *et al.*, *Connected Hybrid Electric Vehicle Simulator*, document C-2019-010781, Korea Copyright Commission, Apr. 2019.

[18] C. Ma, M. Song, S. Choi, K. Jeong, and H. Kim, "Development of efficiency based mode control algorithm for plug-in hybrid electric vehicle," in *Proc. IEEE Vehicle Power Propuls. Conf.*, Daegu, South Korea, Oct. 2012, pp. 1139–1142.

[19] S. Chaker, M. Folie, C. Kehrer, and F. Huber, "Anticipatory shifting-optimization of a transmission control unit for an automatic transmission through advanced driver assistance systems," in *Proc. 11st Int. Modelica Conf.*, Versailles, France, Sep. 2015, pp. 849–854.

[20] D. Kim, "A study on advancement of traffic operating system—V. Methods of adjusting timing of flashing signal for pedestrian," Korea Road Traffic Authority, Wonju, South Korea, Tech. Rep. 1, 2010.

[21] S. Ropelato, F. Zünd, S. Magnenat, M. Menozzi, and R. W. Sumner, "Adaptive tutoring on a virtual reality driving simulator," in *Proc. 10th Int. Workshop Semantic Ambient Media Exper.*, Bangkok, Thailand, Nov. 2017, pp. 12–17.

[22] B. G. Witmer and M. J. Singer, "Measuring presence in virtual environments: A presence questionnaire," *Army Res. Inst. Behav. Social Sci.*, vol. 7, no. 3, pp. 224–240, 1998.

[23] R. S. Kennedy, N. E. Lane, K. S. Berbaum, and M. G. Lilienthal, "Simulator sickness questionnaire: An enhanced method for quantifying simulator sickness," *Int. J. Aviation Psychol.*, vol. 3, no. 3, pp. 203–220, 1993.

[24] E. Ericsson, "Independent driving pattern factors and their influence on fuel-use and exhaust emission factors," *Transp. Res. D, Transp. Environ.*, vol. 6, no. 5, pp. 325–345, 2001.

[25] S. Birrell, J. Taylor, A. McGordon, J. Son, and P. Jennings, "Independent driving pattern factors and their influence on fuel-use and exhaust emission factors," *Transp. Res. D, Transp. Environ.*, vol. 33, pp. 74–86, Dec. 2014.

Kyuhyun Sim received the B.S., M.S., and Ph.D. degrees in mechanical engineering from Sungkyunkwan University, Suwon, South Korea, in 2014, 2016, and 2019, respectively.

He worked as a Research Assistant with the Vehicle Modeling and Simulation Group, Argonne National Laboratory, Lemont, IL, USA, for six months in 2018. He was a Post-Doctoral Researcher in mechanical engineering at Sungkyunkwan University, in 2019. He has been a Senior Research Engineer at Hyundai Motor Company, Hwaseong, South Korea. His research interests include control strategies of hybrid electric vehicles, vehicle dynamics, and powertrain systems.

Sung-Ho Hwang (Member, IEEE) received the B.S., M.S., and Ph.D. degrees in mechanical design and production engineering from Seoul National University, Seoul, South Korea, in 1988, 1990, and 1997, respectively.

From 1992 to 2002, he was a Senior Researcher with the Korea Institute of Industrial Technology, Cheonan. Since 2002, he has been a Professor with the School of Mechanical Engineering, Sungkyunkwan University, Suwon, South Korea. He is the author of two books, more than 100 articles, and more than 20 inventions. His research has focused on fundamental problems of dynamic systems, measurements, and controls in automotive applications, such as powertrain systems, electronic controlled chassis systems, and electric drive systems.

Prof. Hwang served as the Editor-in-Chief of *Journal of Drive and Control* from 2012 to 2016 and the Vice-President at The Korean Society of Automotive Engineers (KSAE) in 2021.